Laser Phys. 27 (2017) 045801 (6pp)
doi:10.1088/1555-6611/aa5c15

Graphene Q-switched Tm:$KY(WO_4)_2$ waveguide laser

E Kifle,[1] X Mateos,[1,2,*] P Loiko,[3] K Yumashev,[4] A Yasukevich,[4] V Petrov,[2] U Griebner,[2] M Aguiló[1] and F Díaz[1]

[1]Física i Cristal·lografia de Materials i Nanomaterials (FiCMA-FiCNA), Universitat Rovira i Virgili (URV), Campus Sescelades, c/ Marcel·lí Domingo, s/n., Tarragona, Spain E-43007
[2]Max-Born-Institute for Nonlinear Optics and Short Pulse Spectroscopy, Max-Born-Str. 2a, Berlin, Germany D-12489
[3]ITMO University, 49 Kronverkskiy pr., St. Petersburg 197101, Russia
[4]Center for Optical Materials and Technologies, Belarusian National Technical University, 65/17 Nezavisimosti Ave., Minsk, Belarus 220013

*Corresponding author: xavier.mateos@urv.cat, mateos@mbi-berlin.de

Abstract We report on the first Tm^{3+}-doped double tungstate waveguide laser passively Q-switched by a graphene saturable absorber using a 12.4 μm-thick 3 at.% Tm:$KY_{0.58}Gd_{0.22}Lu_{0.17}(WO_4)_2$ epitaxial layer grown on a (010)-oriented pure $KY(WO_4)_2$ substrate. This laser generated 5.8 nJ / 195 ns pulses at 1831.8 nm corresponding to a pulse repetition frequency of 1.13 MHz. These are the shortest pulses achieved in passively Q-switched Tm waveguide lasers. The laser slope efficiency was 9% and the Q-switching conversion efficiency reached 45%. Graphene is promising for the generation of ns pulses at ~2 μm in Tm^{3+}-doped double tungstate waveguide lasers operating in the MHz-range.

Keywords: waveguide lasers, thulium, graphene, passive Q-switching.

1. Introduction

In recent years, a lot of attention has been paid to the development of lasers emitting at ~2 μm. Such an emission corresponds to the absorption bands of a number of atmospheric gases (H_2O, CO_2, N_2O) and it is eye-safe. This determines open-space applications of ~2 μm lasers, e.g. in range-finding (LIDAR systems), atmospheric sensing and wind mapping. Strong water absorption at ~2 μm reduces the penetration depth of this radiation into the bio-tissues which is of enormous importance in medicine. The development of ~2 μm lasers with waveguide geometry [1-4] makes them attractive for integrated optics, e.g., for various gas and biomolecule on-chip sensors.

Trivalent Thulium (Tm^{3+}) ions are commonly used to generate ~2 μm laser emission by the $^3F_4 \rightarrow {}^3H_6$ transition [5]. Tm lasers can be efficiently pumped at ~0.8 μm ($^3H_6 \rightarrow {}^3H_4$ absorption band) using commercial high-power AlGaAs laser diodes. An unique feature of the Tm^{3+} ions is the cross-relaxation (CR) process, $^3H_4 + {}^3H_6 \rightarrow {}^3F_4 + {}^3F_4$, which leads to the excitation of two adjacent ions to the upper laser level by the absorption of a single pump photon [5]. The CR process enables a rather high slope efficiency of Tm lasers [6]. In addition, Tm lasers provide broad tuning of the laser emission at ~2 μm.

Monoclinic double tungstates, $KRE(WO_4)_2$ or shortly KREW where RE = Gd, Y or Lu, are very suitable hosts for Tm^{3+} doping and they have been successfully used for the development of efficient bulk and waveguide lasers at ~2 μm [7,8]. Particularly for the waveguide geometry, the concept of "mixed" active layer host, $KGd_xY_yLu_zW$ ($x + y + z = 1$), has been to provide (i) optimum refractive index contrast and (ii) optimum lattice-matching with respect to the undoped substrate, usually KYW, as well as (iii) to ensure high doping levels of active ions [9-11]. High optical quality and low propagation loss (< 0.2 dB/cm) few μm-thick films of $Tm:KGd_xY_yLu_zW$ have been grown on bulk KYW substrates and continuous-wave (CW) [4,6, 12] and passively Q-switched (PQS) [13] laser operation has been reported to date.

Regarding PQS $Tm:KGd_xY_yLu_zW$ waveguide lasers, polycrystalline Cr^{2+}:ZnSe has been used as a saturable absorber (SA). This laser generated 1.2 mW at 1845 nm producing 120 nJ / 1.2 μs pulses at a pulse repetition frequency (PRF) of 7 kHz [13]. The drawback of the Cr^{2+}:ZnSe absorber was its high scattering loss. Carbon nanostructures (graphene and single-walled carbon nanotubes) are emerging in recent years as broadband SAs for bulk and waveguide lasers [14-16]. Graphene, a single layer of carbon atoms arranged in a honeycomb lattice, shows a broadband constant absorption of ~2.3%, ultrafast saturable absorption [17] characterized by low saturation intensity, good thermo-mechanical properties and reasonable laser damage threshold. Due to its special band structure, the graphene-SA is especially suitable for ~2 μm lasers because the saturation intensity at this wavelength (~0.6 MW/cm^2 for ns-pulses) is lower than at ~1 μm [18,19] and, consequently, complete bleaching of the SA can be easily achieved.

Graphene-SAs have been successfully employed for passive Q-switching of bulk lasers at ~2 μm [20-22]. Regarding waveguide lasers, graphene has been mostly studied in ~1 μm PQS oscillators (based on Nd^{3+}- and Yb^{3+}-doped hosts) [16,23]. Two absorber geometries have been studied, the first based on transmission-type SA and the second based on evanescent-field interaction with the SA. At ~2 μm, graphene PQS and Q-switched mode-locked Tm:YAG and Tm:ZBLAN glass waveguides have been studied [24,25]. In the present work, we report on the first graphene PQS Tm double tungstate waveguide laser capable of generating nanosecond pulses at ~2 μm.

2. Experimental

2.1 Waveguides

The studied sample consisted of a bulk undoped KYW substrate, Tm^{3+}-doped lattice-matched active layer and undoped KYW cap layer. At first, the KYW bulk sample was grown

by the Top-Seeded Solution Growth (TSSG) slow-cooling method. It was cut parallel to the (010) natural face and polished with very high quality. The active layer had a composition of $KY_{0.58}Gd_{0.22}Lu_{0.17}Tm_{0.03}W$. It was grown by the Liquid Phase Epitaxy (LPE) method from a solution with a molar ratio solute/solvent of 7/93. Potassium ditungstate, $K_2W_2O_7$, was used as a solvent. The reagents K_2CO_3, Gd_2O_3, Y_2O_3, Lu_2O_3, WO_3, Tm_2O_3 and Ho_2O_3 (Sigma-Aldrich) used were with 99.9% purity. The growth of the active layer was carried out for 5 h at 4 K below the saturation temperature, T_s = 1173 K. The actual Tm concentration in the active layer was determined by Electron Probe MicroAnalysis (EPMA), $N_{Tm} = 1.75\times10^{20}$ cm^{-3} (3 at%). The as-grown active layer was ~80 μm thick. It was polished down to 12.4 μm. On the active layer, a cap layer of undoped KYW was grown by LPE. After polishing it, the thickness of this layer amounted to 58 μm. The fabricated sample (we will refer to it further as Tm:KYW waveguide) was oriented for light propagation along the N_g axis of the optical indicatrix. The refractive index contrast between the active layer and substrate and cap layer was estimated from the available Sellmeier equations [11], which were fitted to measurements with an accuracy of Δn ~0.002 at the laser wavelength. Both N_g-faces of the sample were polished to laser quality, resulting in a length of 5.0 mm. An Environmental Scanning Electron Microscope (ESEM, Quanta 200 ESEM model) back-scattering image obtained for the polished end-face of the sample is shown in figure 1.

2.2 Laser set-up

The scheme of the laser set-up is shown in figure 2(a). The Tm:KYW waveguide sample was placed on a passively-cooled glass substrate. The laser cavity consisted of a flat pump mirror (PM) that was antireflection (AR) coated for 0.7–1 μm and high-reflection (HR) coated for 1.8–2.1 μm and a flat output coupler (OC) providing a transmission of T_{OC} = 5% at 1.8–2.1 μm. A transmission-type graphene SA was inserted between the waveguide and OC. All elements in the cavity were placed as close as possible.

As a pump source, we used a Ti:Sapphire laser (Coherent, model MIRA 900) tuned to 802 nm ($^3H_6 \rightarrow {}^3H_4$ transition of Tm^{3+} ions). The polarization of the pump beam was adjusted to be along the N_m-axis of the active layer. The pump light was coupled into the waveguide with a 10x microscope objective lens (NA: 0.28, focal length: 20 mm). The incident pump power was varied with a gradient neutral density filter placed in front of the objective. The pump beam radius in the focus was 32 μm. The measured small-signal pump absorption was ~70% and the absorption dropped to ~60% for the highest pump power. The efficiency of the pump light coupling into the waveguide was estimated from the geometrical overlap of the pump beam and the active layer cross-section to be ~24%. The waveguide laser signal was separated from the pump with a cut-off filter and collimated with a 40 mm aspheric lens. Pumping of the waveguide resulted in a bright bluish upconversion, figure 2(b).

The emission wavelength was detected with an optical spectrum analyzer (Yokogawa AQ6375). The far-field profile of the guided mode was analyzed using a FIND-R-SCOPE near IR camera. A fast InGaAs photodiode (rise time: 200 ps) and a 2 GHz digital oscilloscope were used for recording the Q-switched pulses.

2.3 Saturable absorber

A commercial transmission-type single-layer graphene (Supermarket graphene) was employed. It was fabricated by the chemical vapour deposition (CVD) method and deposited on a 1.05 mm-thick uncoated fused silica substrate. The initial (small-signal) transmission of the graphene layer at ~2.06 μm was 97.7%, determined as *T*(graphene+substrate) / *T*(substrate), see figure 3(a). The number of graphene layers (one) was confirmed by Raman spectroscopy with the ratio (~0.2) between the integral intensities of the G and 2D Raman bands, see figure 3(b). According to our previous studies, the saturation intensity of the studied

graphene for ns pulse duration is I_{sat} = 0.6 MW/cm^2 and the saturable absorption α'_S = 0.12% [22].

3. Results and discussion

At first, we studied the CW laser performance of the Tm:KYW waveguide (with the SA removed from the cavity), see figure 4. This laser generated 14.4 mW at 1835.4 nm with a slope efficiency η of 18% with respect to the absorbed pump power. Lasing occurred at a threshold of P_{abs} = 38 mW.

Stable passive Q-switching was achieved when inserting the graphene-SA in the cavity. The maximum average output power reached 6.5 mW at a wavelength of 1831.8 nm corresponding to η = 9%, figure 4. The laser threshold was at P_{abs} = 51 mW. The conversion efficiency with respect to the CW operation mode η_{opt} reached 45%. The blue-shift of the emission wavelength for the PQS laser is explained by increased intracavity losses due to the insertion of the graphene-SA and it is typical for quasi-three-level Tm^{3+} lasers. For both CW and PQS regimes, the laser output was linearly polarized ($E \parallel N_m$). The output beam of the laser was multimode and strongly elliptic, see inset in figure 4(a). According to the dispersion relation [26], the studied waveguide supports two transversal electric (TE) guided modes in the vertical direction, namely for m = 0 (TE_0) and m = 1 (TE_1) at a wavelength of ~1.84 μm.

The dependence of the pulse characteristics (pulse duration, $\Delta\tau$, determined as full width at half maximum, FWHM, pulse repetition frequency, PRF, pulse energy, $E_{out} = P_{out}$/PRF, and peak power, $P_{peak} = E_{out}/\Delta\tau$), are shown in figure 5. When the absorbed pump power increased from 75 to 126 mW, the pulse duration shortened from 312 to 195 ns and the pulse energy increased from 2.3 to 5.8 nJ. This was accompanied by a nearly linear increase of the PRF, in the range 0.73-1.13 MHz. The maximum peak power reached ~30 mW.

The output characteristics of the graphene-SA PQS Tm:KYW laser were modeled with a "fast" SA model, see details in [19,22]. The parameters of the active material [7,11,12] and the SA [22] used for the calculations are summarized in table 1. Here for the active layer, we used the spectroscopic parameters reported previously for Tm:KLuW [7]. The results of the modeling are presented in figure 5 as solid curves. The modelling shows a very good agreement with the experimental data. At P_{abs} = 126 mW, it predicts the generation of 7 nJ / 215 ns pulses at PRF = 1.16 MHz. The round-trip resonator loss estimated from the modelling is ~7%.

The oscilloscope trace of the shortest single Q-switched pulse and the corresponding pulse train are shown in figure 6. The intensity instabilities in the pulse train are <10% and the rms pulse-to-pulse timing jitter is <15%. The Q-switching instabilities in the studied laser are caused mainly by the temporal fluctuations in the output of the Ti:Sapphire laser and to less extend – to the heating of the graphene-SA by the non-absorbed pump [20]. No damage of the graphene-SA was observed while the long-term stability of the PQS laser was limited by the above-mentioned fluctuations of the Ti:Sapphire laser. The calculated pulse train corresponding to P_{abs} = 126 mW is shown in figure 7. It agrees well with the experimental data.

A comparison of the output characteristics of the PQS Tm waveguide lasers reported so far is presented in table 2. The pulse duration achieved with the present graphene-SA PQS Tm:KYW laser is much shorter than in the previous reports.

Future work with graphene PQS Tm^{3+}-doped double tungstate waveguide lasers should focus on the channel waveguide geometry. Channel waveguides can be fabricated either by microstructuring of a planar waveguide prepared by LPE, or by direct writing in a bulk Tm^{3+}-doped crystal with a femtosecond laser. The latter can be done in crystals with a conventional composition, e.g. Tm:KLuW. In addition, an increase of the Tm doping level to >5 at.% is desirable to reach a laser quantum efficiency of >1.95 owing to an efficient CR [6]. This will increase the laser slope efficiency and allow for further power scaling, as well as provide much better conditions for the bleaching of the graphene-SA due to a much smaller size of the laser mode.

The direct deposition of graphene on the waveguide end-face will ultimately reduce the SA insertion losses. Further shortening of the pulse duration and scaling of the pulse energy is expected when using the SA with higher modulation depth, e.g. containing several graphene layers. However, this layer stacking might lead to increased scattering on the layer-to-layer interfaces and, consequently, larger fraction of non-saturable losses. In this way, different nanostructured SAs, e.g. based on single-walled carbon nanotubes [22] or few-layer MoS_2 [27], which are known for their relatively low non-saturable losses, could be an alternative.

4. Conclusion

We report on the first ~2 μm double tungstate waveguide laser passively Q-switched by a graphene-SA. The laser is based on a buried 3 at.% Tm^{3+}-doped $KY_{0.58}Gd_{0.22}Lu_{0.17}W$ lattice-matched active layer grown on an undoped (010)-oriented KYW substrate. It generates 5.8 nJ / 195 ns pulses at a pulse repetition frequency as high as 1.13 MHz and at a wavelength of 1831.8 nm. This represents the shortest pulse duration achieved with PQS 2 μm waveguide lasers. The Q-switching conversion efficiency reached 45%. The graphene-SA is very promising for the generation of sub-100 ns pulses in the MHz-range if employed in channel Tm^{3+}-doped double tungstate waveguide lasers. A recent demonstration of Ho^{3+} lasing in a Tm,Ho-codoped double tungstate waveguide [28] may enable the generation of ns pulses at wavelengths longer than ~2 μm. Indeed, graphene PQS of a bulk Tm,Ho:KLuW laser has been already demonstrated [29].

Acknowledgments

This work was supported by the Spanish Government (projects MAT2016-75716-C2-1-R, MAT2013-47395-C4-4-R and TEC2014-55948-R) and Generalitat de Catalunya (project 2014SGR1358). F.D. acknowledges additional support through the ICREA academia award 2010ICREA-02 for excellence in research. This work has received funding from the European Union's Horizon 2020 research and innovation programme under grant agreement No 654148 Laserlab-Europe and under the Marie Skłodowska-Curie grant agreement No 657630. P. Loiko acknowledges financial support from the Government of the Russian Federation (Grant 074-U01) through ITMO Post-Doctoral Fellowship scheme.

References

[1] Sheperd D P, Brinck D J B, Wang A, Tropper A C, Hanna D C, Kakarantzas G and Townsend P D 1994 *Opt. Lett.* **19** 954-6.

[2] Lancaster D G, Gross S, Ebendorff-Heidepriem H, Kuan K, Monro T M, Ams M, Fuerbach A and Withford M J 2011 *Opt. Lett.* **36** 1587-9.

[3] Mackenzie J I, Mitchell S C, Beach R J, Meissner H E and Shepherd D P 2001 *Electron. Lett.* **37** 898-9.

[4] Rivier S, Mateos X, Petrov V, Griebner U, Romanyuk Y E, Borca C N, Gardillou F and Pollnau M 2007 *Opt. Express* **15** 5885-92.

[5] Stoneman R C and Esterowitz L 1990 *Opt. Lett.* **15** 486–8.

[6] van Dalfsen K, Aravazhi S, Grivas C, García-Blanco S M and Pollnau M 2014 *Opt. Lett.* **39** 4380-3.

[7] Petrov V, Pujol M C, Mateos X, Silvestre Ò, Rivier S, Aguiló M, Solé R, Liu J, Griebner U and Díaz F 2007 *Laser & Photonics Rev.* **1** 179-212.

[8] Pollnau M, Romanyuk Y E, Gardillou F, Borca C N, Griebner U, Rivier S and Petrov V 2007 *IEEE J. Select. Top. Quantum Electron*. **13** 661-71.

[9] Silvestre Ò, Aznar A, Solé R, Pujol M C, Díaz F and Aguiló M 2008 *J. Phys.: Cond. Matter* **20** 225004-1-10.

[10] Bolaños W, Carvajal J J, Pujol M C, Mateos X, Lifante G, Aguiló M and Díaz F 2009 *Cryst. Growth & Design* **9** 3525-31.

[11] Aravazhi S, Geskus D, van Dalfsen K, Vazquez-Cordova S A, Grivas C, Griebner U, Garcia-Blanco S M and Pollnau M 2013 *Appl. Phys. B* **111** 433-46.
[12] van Dalfsen K, Aravazhi S, Grivas C, García-Blanco S M and Pollnau M 2012 *Opt. Lett.* **37** 887-9.
[13] Bolaños W, Carvajal J J, Mateos X, Cantelar E, Lifante G, Griebner U, Petrov V, Panyutin V L, Murugan G S, Wilkinson J S, Aguiló M and Díaz F 2011 *Opt. Express* **19** 1449-54.
[14] Cho W B, Yim J H, Choi S Y, Lee S, Schmidt A, Steinmeyer G, Griebner U, Petrov V, Yeom D-I, Kim K and Rotermund F 2010 *Adv. Funct. Mater.* **20** 1937-43.
[15] Bao Q, Zhang H, Wang Y, Ni Z, Yan Y, Shen Z X, Loh K P and Tang D Y 2009 *Adv. Funct. Mater.* **19** 3077–83.
[16] Choudhary A, Beecher S J, Dhingra S, D'Urso B, Parsonage T L, Grant-Jacob J A, Hua P, Mackenzie J I, Eason R W and Shepherd D P 2015 *Opt. Lett.* **40** 1912-5.
[17] Xing G, Guo H, Zhang X, Sum T C and Huan C H A 2010 *Opt. Express* **18** 4564-73.
[18] Zhang F, Han S, Liu Y, Wang Z and Xu X 2015 *Appl. Phys. Lett.* **106** 091102-1–5.
[19] Loiko P A, Serres J M, Mateos X, Liu J, Zhang H, Yasukevich A S, Yumashev K V, Petrov V, Griebner U, Aguiló M and Díaz F 2016 *Appl. Phys. B* **122** 105-1-8.
[20] Serres J M, Loiko P, Mateos X, Yumashev K, Griebner U, Petrov V, Aguiló M and Díaz F 2015 *Opt. Express* **23** 14108-13.
[21] Xie G Q, Ma J, Lv P, Gao W L, Yuan P, Qian L J, Yu H H, Zhang H J, Wang J Y and Tang D Y 2012 *Opt. Mater. Express* **2** 878-83.
[22] Lan R, Loiko P, Mateos X, Wang Y, Li J, Pan Y, Choi S Y, Kim M H, Rotermund F, Yasukevich A, Yumashev K, Griebner U and Petrov V 2016 *Appl. Opt.* **55** 4877–87.
[23] Tan Y, Cheng C, Akhmadaliev S, Zhou S and Chen F 2014 *Opt. Express* **22**, 9101–6.
[24] Lee J H, Gross S, Cunning B V, Brown C L, Kielpinski D, Monro T M and Lancaster D G, in *CLEO, San Jose, 8–13 June 2014* (OSA, 2014), P. JTu4A.128.
[25] Ren Y Y, Beecher S J, Brown G, Ródenas A, Lancaster A, Chen F and Kar A K, in *CLEO Pacific Rim, Kyoto, 30 June-4 July 2013* (IEEE, 2013), P. ThA1-3.
[26] Tien P K and Ulrich R 1970 *J. Opt. Soc. Am.* **60** 1325-37.
[27] Serres J M, Loiko P, Mateos X, Yu H, Zhang H, Chen Y, Petrov V, Griebner U, Yumashev K, Aguiló M and Díaz F 2016 *Opt. Mater. Express* **6** 3262–3273.
[28] Ruiz Madroñero C V, Mateos X, Loiko P, Petrov V, Griebner U, Aguiló M and Díaz F 2016 *Laser Phys. Lett.* **13** 095801-1–6.
[29] Serres J M, Loiko P, Mateos X, Jambunathan V, Yumashev K, Griebner U, Petrov V, Aguiló M and Díaz F 2016 *Laser Phys. Lett.* **13** 025801-1-5.

Table 1 Material properties of the active layer (at a wavelength of 1.84 μm, for light polarization $E \parallel N_m$, where applicable) and graphene-SA used for the modelling of the Q-switched laser performance.

Parameter	Notation	Value
Active layer, "mixed" Tm:KYW		
Tm^{3+} concentration	N_{Tm}	1.75×10^{20} cm^{-3}
Absorption cross-section [7]	σ^{p}_{abs}	5.2×10^{-20} cm^2
SE cross-section [7]	σ^{L}_{SE}	2.6×10^{-20} cm^2
Reabsorption cross-section [7]	σ^{L}_{abs}	1.0×10^{-20} cm^2
Lifetime of Tm^{3+} [7]	$\tau(^3F_4)$	0.8 ms
Quantum efficiency [12]	η_q	1.66
Refractive index [11]	n_{AM}	1.995
Length	t_{AM}	5.0 mm
Graphene-SA		
Initial absorption	α'	2.3%
Saturable absorption [22]	α'_S	0.12%
Saturation intensity [22]	I_{sat}	0.6 MW/cm^2
Refractive index (SiO_2)	n_{SA}	1.439
Thickness	t_{SA}	1.05 mm

Table 2 Summary of the PQS Tm-doped waveguide lasers reported so far.

Gain material	Geometry / fabrication*	SA	P_{out}, mW	τ, ns	E_{out}, nJ	PRF, kHz	P_{peak}, mW	Ref.
Tm:KYW	planar / LPE	graphene	6.5	195	5.8	1130	30	This work
Tm:KYW	planar / LPE	Cr^{2+}:ZnS	1.2	1200	120	10	100	[13]
Tm:ZBLAN	channel / fs	graphene	6	1400	240	25	170	[24]
Tm:YAG	channel / fs	graphene	6.5	<500	9.5	684	~20	[25]

*LPE – liquid-phase epitaxy, fs – femtosecond-written.

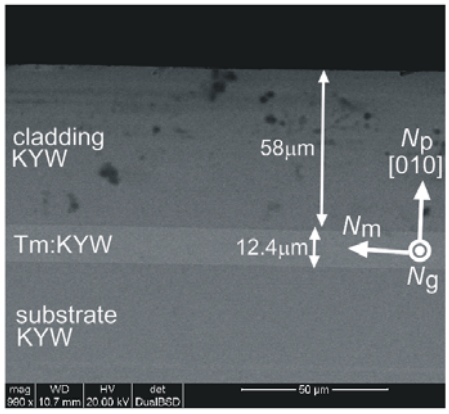

Figure 1 Backscattering ESEM image of a polished end-facet of a Tm:KYW planar waveguide.

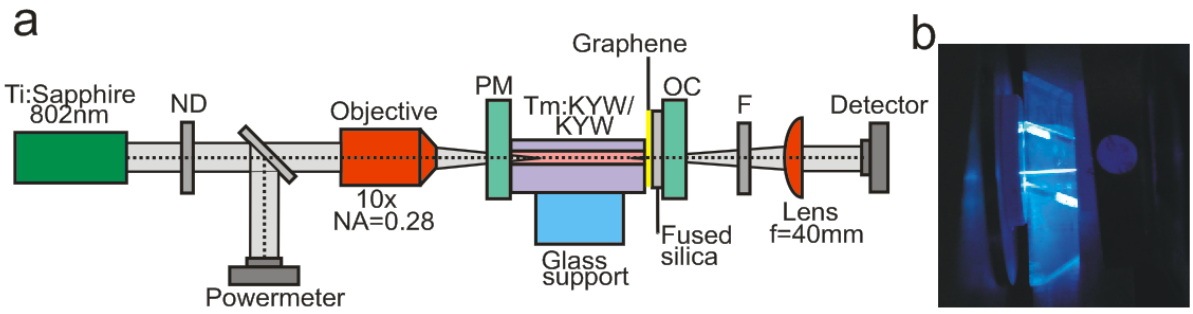

Figure 2 (a) Experimental set-up: ND - neutral density filter, PM - pump mirror, OC - output coupler, F - cut-on filter; (b) Blue upconversion in the Tm:KYW waveguide.

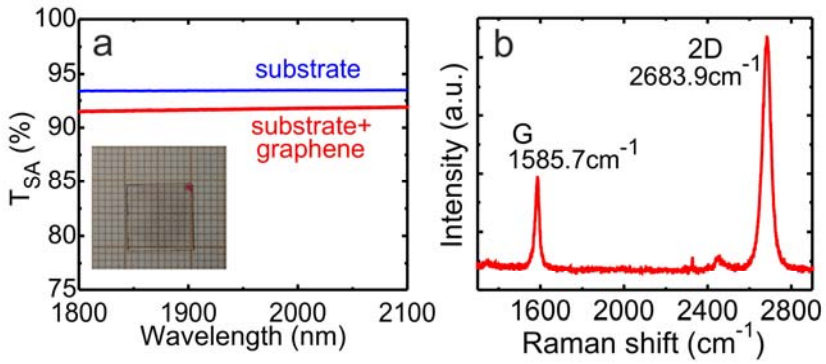

Figure 3 Graphene-SA: (a) absorption spectrum, *inset*: image of the SA; (b) Raman spectrum.

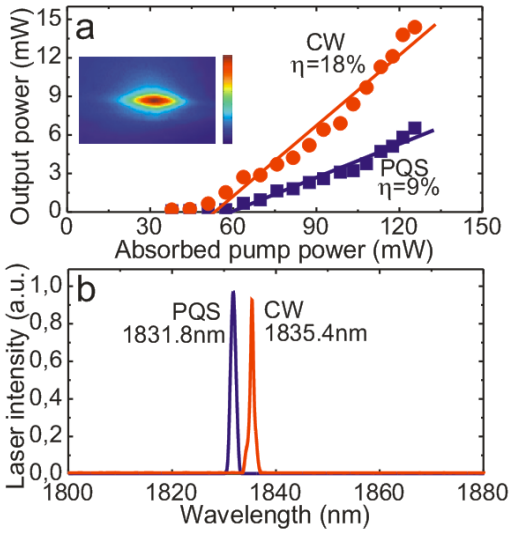

Figure 4 CW and graphene PQS Tm:KYW waveguide lasers: (a) input-output dependences, η - slope efficiency, *inset* - spatial profile of the laser beam; (b) typical laser emission spectra measured at P_{abs} = 126 mW.

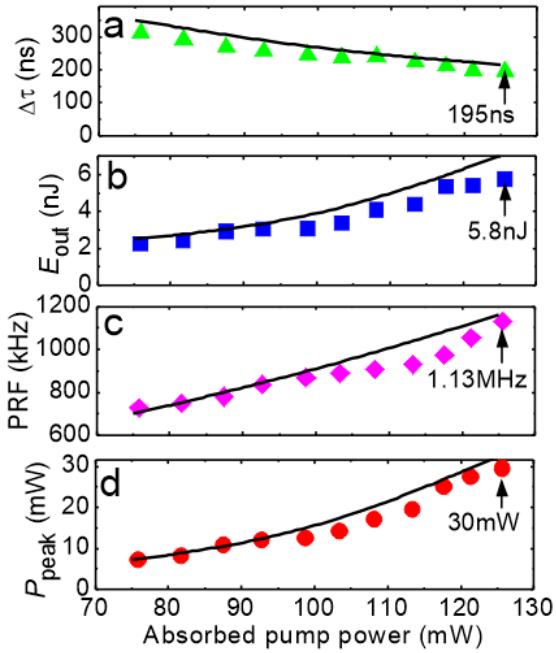

Figure 5 Graphene PQS Tm:KYW waveguide laser: (a) pulse duration $\Delta\tau$ (FWHM), (b) pulse energy E_{out}, (c) pulse repetition frequency (PRF) and (d) peak power P_{peak} versus the absorbed pump power: *symbols* – experimental data, *curves* – modelling.

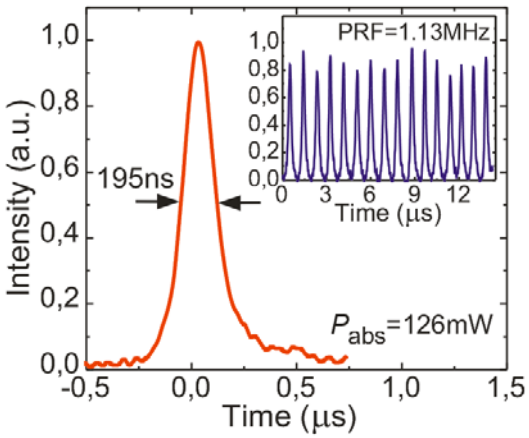

Figure 6 Oscilloscope trace of a single Q-switched pulse and the corresponding pulse train (inset) for graphene PQS Tm:KYW waveguide laser, P_{abs} = 126 mW.

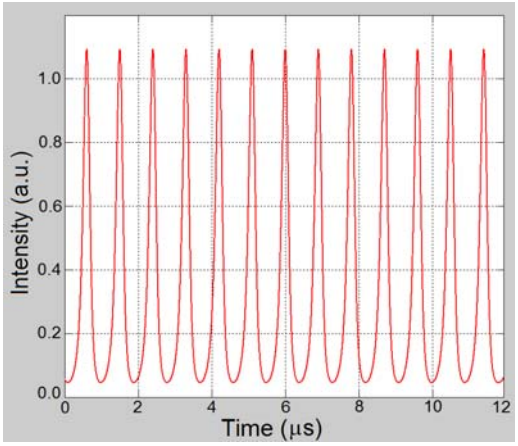

Figure 7 Calculated pulse train for a graphene PQS Tm:KYW waveguide laser using the parameters listed in Table 1, at P_{abs} = 126 mW.